Differential Modulation for Cooperative Wireless Systems

Qiang Zhao and Hongbin Li, *Member, IEEE*

Abstract—This paper examines differential binary modulation for wireless networks that utilize wireless relays to seek cooperative diversity and improved performance. Two differential cooperative transmission schemes, referred to as *differential amplify-and-forward* (DAF) and *differential decode-and-forward* (DDF), respectively, are introduced. These schemes require no channel state information at any node in the system. A set of analytical results pertaining to the probability density function of the instantaneous signal-to-noise ratio, average bit error rate, outage probability, and diversity order of the proposed schemes in Rayleigh fading channels are obtained. The analytical results are confirmed by numerical simulations. It is shown that the differential cooperative DAF and DDF schemes achieve cooperative diversity and outperform the conventional noncooperative differential modulation.

Index Terms—Average bit error rate (BER), cooperative diversity, differential modulation, outage probability, wireless relays.

I. INTRODUCTION

DIVERSITY provides an effective mechanism to combat multipath-induced fading in wireless communication systems. Among various diversity techniques, spatial diversity derived from multiantenna transmission/reception has received widespread interest in recent years. However, multiple antennas may be unavailable in some systems, e.g., the mobile terminals of cellular networks, mobile ad-hoc networks, and wireless sensor networks, due to size, power, and cost limitations. In such cases, *cooperative diversity*, which relies on cooperation among multiple spatially distributed nodes, provides a useful alternative for fading mitigation. Specifically, owing to the broadcasting nature of the wireless medium, transmission from a source node may be heard by nodes in the neighborhood. These neighbor nodes may act as *wireless relays* and provide alternative communication routes that give rise to cooperative diversity.

A. Prior Related Research

Cooperative diversity has root in classical work on relay channels (e.g., [1] and [2]). Practical cooperative techniques were first proposed and investigated in [3] and [4]. It was shown

that cooperative diversity increases the achievable rate region over noncooperative schemes in ergodic fading channels, providing that the channel state information (CSI) is known to the transmitters and receivers. Several low-complexity cooperative transmission schemes based on half-duplex operation were discussed in [5], including the *amplify-and-forward* (AF) scheme by which relays amplify the received signal subject to a power constraint and retransmit it to the destination, the *decode-and-forward* (DF) scheme that performs hard decisions at the relays before retransmission, and a few other cooperative schemes that utilize selection or incremental relaying. Outage capacity and diversity of these cooperative schemes when the CSI is known only at the receivers in delay-limited scenarios were also examined in [5]. Coherent maximum likelihood (ML) detectors for AF and DF were developed in [6].

Along the line of end-to-end performance analysis, the average bit error rate (BER) and outage probability of a two-hop, single-relay system were examined in [7] for Rayleigh fading and in [8] for Nakagami fading. The two-hop system assumes no direct transmission from the source to destination and, thus, provides no diversity. A closed-form asymptotic (for high SNR) approximation of the average symbol error rate for multibranch multihop systems using AF was obtained in [9]. It was shown there that the optimum location for the relay is at the mid-point between the source and destination. Meanwhile, Chen and Laneman recently considered ML detection for noncoherent binary phase-shift keying (BFSK) and computed the associated average BER and diversity [10].

B. Motivation and Contributions

With the exception of the noncoherent scheme in [10], most of the aforementioned studies focused on coherent detection, assuming the CSI can be reliably estimated at the relays and destination nodes, either by training or blind estimation techniques. However, channel estimation is known to be a challenging and costly task, especially in time-selective fading environments. The difficulty is exacerbated in multiantenna or multinode wireless systems since the amount of training or convergence time (incurred by blind techniques) grows with the number of links. The need for differential or noncoherent modulation techniques to circumvent channel estimation in multiantenna systems has been well recognized (e.g., [11]). It is imperative to develop these techniques for cooperative multinode wireless systems since their burden of channel estimation is even more severe than multiantenna systems. Specifically, a multiantenna system with L transmit and one receive antennas involves L wireless channels. In contrast, a cooperative system with one source, $L - 1$ relays, and one destination node has a total of $2L - 1$
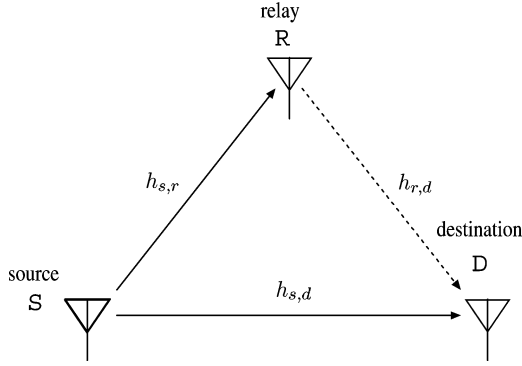
Fig. 1. Cooperative wireless relay system.

fading channels that connect the source to the destination and relays, respectively, and the relays to the destination.

Following the preliminary investigation in [12], we provide in this paper a more comprehensive study on differential modulation for cooperative wireless systems. We consider an uncoded system with one source S, one relay R, and one destination D, as depicted in Fig. 1. A summary of our contributions are the following.

1) We consider two differential modulation based cooperative schemes, namely *differential amplify-and-forward* (DAF) and *differential decode-and-forward* (DDF), which are amenable to differential detection in fading channels.

2) For the DAF scheme, we derive linear combiners for combining at the destination. Assuming Rayleigh fading channels, we compute a closed-form expression for the probability density function (PDF) of the *instantaneous SNR* of the relay link (*viz.*, S—R—D link), and obtain a closed-form expression of the *average BER* when only the relay link is used for detection, which would be of interest in scenarios where S cannot reach D directly due to power limitation. When both the relay link and direct link (*viz.*, S—D link) are combined for detection, we derive a good approximation of the average BER. We also find the *outage probability* of the DAF scheme in Rayleigh fading.

3) For the DDF scheme, the ML detector is shown to take a nonlinear form due to possible decision errors occurred at R. The nonlinearity complicates the implementation of the ML detector, while making analysis intractable. Using a piecewise-linear (PL) approximation of the nonlinear decision function first observed in [6], we obtain a PL detector which is shown to closely match the ML detector. Average BER analysis for the PL detector is pursued in two approaches. The first yields an *exact* expression of the average BER expressed in series expansion. The second leads to an *approximate* expression of the average BER obtained by high SNR approximation. Both are found to be accurate predictions of average BER over a wide range of SNR. The outage probability pertaining to the DDF is computed in closed-form.

4) We study the diversity of DAF and DDF by examining the asymptotic behaviors of their average BER and outage probability. It is found that both yield full diversity as the SNR increases without bound.

The rest of this paper is organized as follows. Section II describes the system model. The proposed DAF and DDF schemes along with their differential detection techniques are detailed in Section III. Analytical results are presented in Section IV. Section V contains simulation results. Finally, we provide concluding remarks in Section VI.

II. SYSTEM MODEL

Consider a wireless relay network depicted in Fig. 1 that is composed of one source S, one relay R and one destination D node, where a sequence of symbols are to be transmitted from S to D. To eliminate mutual interference, S and R use orthogonal channels for transmission, either by time-, frequency-, or code-division multiplexing. For ease of presentation, we assume time-division multiplexing by which the transmission is divided into *two* distinct phases as in [5]. During *phase-I* transmission, S transmits a frame of information bits, while R and D listen. During *phase-II* transmission, S is silent, while R amplifies or decodes the received signal, and retransmits it to D.

For phase-I transmission, considering binary phase shift keying (BPSK) constellation, the information bits $d(n) \in \{\pm 1\}$ at S are differentially encoded

$$s(n) = s(n-1)d(n), \quad n = 1, 2, \cdots, N \qquad (1)$$

where $s(n)$ denotes the signal transmitted from S, $s(0) = 1$ is the initial reference bit, and N is the number of bits within one frame. The baseband signals received at R and D, respectively, are

$$x_r(n) = h_{s,r}s(n) + w_r(n), \quad n = 0, 1, \cdots, N \qquad (2)$$
$$x_d(n) = h_{s,d}s(n) + w_d(n), \quad n = 0, 1, \cdots, N \qquad (3)$$

where $h_{s,r}$ and $h_{s,d}$ denote the corresponding fading coefficients, while $w_r(n)$ and $w_d(n)$ denote the channel noise.

For phase-II transmission, relay R amplifies or decodes (see Section III for details) the received signal $x_r(n)$, and generates a *unit-variance* signal $s_r(n)$ that is transmitted to destination D. The signal received at D is given by[1]

$$y_d(n) = h_{r,d}s_r(n) + u_d(n), \quad n = 0, 1, \cdots, N \qquad (4)$$

where $h_{r,d}$ and $u_d(n)$ denotes the fading and channel noise, respectively.

For differential detection, the fading channels are assumed (approximately) static over two bit intervals. The dependence of the channels on time is dropped for brevity since the detection schemes to be discussed in Section III involve signals received over two adjacent bits. The channels are Rayleigh fading, i.e., $h_{i,j} \sim \mathcal{CN}(0, \sigma_{i,j}^2)$, $(i,j) \in \{(s,r), (s,d), (r,d)\}$, where $\mathcal{CN}(\mu, \sigma^2)$ denotes a complex Gaussian random variable with mean μ and variance σ^2. The channel noise $w_r(n)$, $w_d(n)$, and $u_d(n)$ are assumed independent $\mathcal{CN}(0, N_0)$ random variables. The *instantaneous SNR* between nodes i and j, denoted by $\gamma_{i,j} = |h_{i,j}|^2/N_0$, is exponentially distributed with PDF

$$p_{\gamma_{i,j}}(\gamma_{i,j}) = \frac{1}{\bar{\gamma}_{i,j}} e^{-\gamma_{i,j}/\bar{\gamma}_{i,j}} \qquad (5)$$

[1]With some notation abuse, n denotes the time index for both phase-I and phase-II transmissions.

where $\bar{\gamma}_{i,j} = \sigma_{i,j}^2/N_0$ denotes the *average SNR* between nodes i and j. Finally, the channel fading coefficients are assumed independent of one another and also of the channel noise.

III. PROPOSED SCHEMES

A. DAF Scheme

1) DAF Transmission at R: For phase-II transmission, the signal received at R in phase-I is amplified or scaled to meet an average power constraint

$$s_r(n) \triangleq \frac{x_r(n)}{(\text{var}\{x_r(n)\})^{1/2}} = \frac{x_r(n)}{\left(N_0 + \sigma_{s,r}^2\right)^{1/2}}. \tag{6}$$

Clearly, $s_r(n)$ has unit average power. Note that our DAF scheme (6) differs from the AF scheme in [5] for *coherent* modulation

$$s_r(n) = \frac{x_r(n)}{(N_0 + |h_{s,r}|^2)^{1/2}}. \tag{7}$$

Specifically, (7) requires the magnitude of the *instantaneous* channel $h_{s,r}$, which is difficult to obtain in time-selective fading channels. Meanwhile, $\text{var}\{x_r(n)\}$ in (6) can be conveniently estimated by time-averaging over a frame of received signals. Hence, (6) is more suitable for *differential* modulation, while (7) is more appropriate for coherent modulation.

2) Differential Detection at D: Substituting (2) and (6) into (4) yields

$$y_d(n) = \tilde{h}_{s,d}s(n) + \tilde{w}_d(n), \quad n = 0, 1, \cdots, N \tag{8}$$

where $\tilde{h}_{s,d}$ is the *effective channel gain* of the relay link (S−R−D)

$$\tilde{h}_{s,d} \triangleq \frac{h_{s,r}h_{r,d}}{\left(N_0 + \sigma_{s,r}^2\right)^{1/2}} \tag{9}$$

while $\tilde{w}_d(n)$ is the *effective channel noise*

$$\tilde{w}_d(n) \triangleq \frac{h_{r,d}}{\left(N_0 + \sigma_{s,r}^2\right)^{1/2}}w_r(n) + u_d(n) \tag{10}$$

whose conditional distribution is

$$\mathcal{CN}(0, |h_{r,d}|^2 N_0(N_0 + \sigma_{s,r}^2)^{-1} + N_0)$$

given $h_{r,d}$.

Differential detection using only (3) in the direct link (S−D) or only (8) in the relay link (S−R−D) is standard. Of more interest is to use both links to seek additional diversity gain. From (1) and (3), $x_d(n)$ can be rewritten as

$$x_d(n) = x_d(n-1)d(n) + v(n) \tag{11}$$

where $v(n) \triangleq w_d(n) - w_d(n-1)d(n)$. Clearly, we have $x_d(n) \sim \mathcal{CN}(x_d(n-1)d(n), 2N_0)$ conditioned on the information bit $d(n)$ and the previous received signal $x_d(n-1)$. Likewise, using (1) and (8), we have

$$y_d(n) = y_d(n-1)d(n) + \tilde{v}(n) \tag{12}$$

where $\tilde{v}(n) \triangleq \tilde{w}_d(n) - \tilde{w}_d(n-1)d(n)$, which indicates that $y_d(n) \sim \mathcal{CN}(y_d(n-1)d(n), 2|h_{r,d}|^2 N_0 (N_0 + \sigma_{s,r}^2)^{-1} + 2N_0)$ given $y_d(n-1)$, $h_{r,d}$, and $d(n)$.

Equations (11) and (12) are the fundamental differential equations for DAF, which relate the outputs of the direct and relay links to the input $d(n)$ without explicit dependence on the unknown channels. Note that $x_d(n)$ and $y_d(n)$ are independent and conditional Gaussian random variables. We can follow a maximum likelihood approach by using the joint PDF of $x_d(n)$ and $y_d(n)$, which yields the following linear combiner:

$$z(n) = x_d^*(n-1)x_d(n) + \frac{1 + \bar{\gamma}_{s,r}}{1 + \bar{\gamma}_{s,r} + \gamma_{r,d}}y_d^*(n-1)y_d(n) \tag{13}$$

where $(\cdot)^*$ denotes complex conjugation. The above combiner, which applies different weights for the two branches, differs from the standard linear combiner [13, (14.4-23)] for multichannel differential communications because the noise power for the two branches is different. Since (13) requires knowledge of instantaneous SNR $\gamma_{r,d}$, it is not suitable for differential detection. A differential combiner can be obtained by replacing $\gamma_{r,d}$ with its average

$$z(n) = x_d^*(n-1)x_d(n) + \frac{1 + \bar{\gamma}_{s,r}}{1 + \bar{\gamma}_{s,r} + \bar{\gamma}_{r,d}}y_d^*(n-1)y_d(n). \tag{14}$$

Simulation results in Section V show that (13) and (14) yield similar BER performance. Finally, the information bits are detected as follows:

$$\hat{d}(n) = \text{sign}\left(\Re\{z(n)\}\right) \tag{15}$$

where $\Re\{\cdot\}$ denotes the real part of the argument.

B. DDF Scheme

1) DDF Transmission at R: At relay R, the received signal is first differentially decoded as follows:

$$\tilde{d}(n) = \text{sign}\left(\Re\{x_r^*(n-1)x_r(n)\}\right) \quad n = 1, 2, \cdots, N. \tag{16}$$

Next, the decoded bits are re-encoded via a differential encoder

$$s_r(n) = s_r(n-1)\tilde{d}(n), \quad n = 1, 2, \cdots, N \tag{17}$$

with $s_r(0) = 1$. Finally, $s_r(n)$ is transmitted to destination D during phase-II.

2) Differential Detection at D: Substituting (17) into (4), we have

$$y_d(n) = y_d(n-1)\tilde{d}(n) + \tilde{v}(n) \tag{18}$$

where $\tilde{v}(n) \triangleq u_d(n) - u_d(n-1)\tilde{d}(n)$ whose conditional distribution is $\mathcal{CN}(0, 2N_0)$. Since relay D makes hard decoding in (16), either a correct or wrong decision may occur. As a result, the conditional PDF of $y_d(n)$ takes the form of Gaussian mixture

$$p_{y_d(n)}(y) = (1 - \epsilon)\Phi_c\left(y; y_d(n-1)d(n), 2N_0\right)$$
$$+ \epsilon\Phi_c\left(y; -y_d(n-1)d(n), 2N_0\right) \tag{19}$$

where $\Phi_c(y; \mu, \sigma^2)$ denotes the PDF of a complex Gaussian random variable with mean μ and variance σ^2, and ϵ is the av-

erage BER of differential BPSK in Rayleigh fading channels [13, (14.3-10)]

$$\epsilon = \frac{1}{2 + 2\bar{\gamma}_{s,r}} \tag{20}$$

which is also the average probability with which relay R makes an error in each decision.

The fundamental differential equations for DDF are (11) and (18). Note that $x_d(n)$ and $y_d(n)$ are independent. Due to the mixture distribution shown in (19), the ML detector takes a nonlinear form. Specifically, by using the joint PDF of $x_d(n)$ and $y_d(n)$ and following a similar procedure as in [6], we have the following *ML detector* for DDF

$$f(t_1) + t_0 \underset{-1}{\overset{1}{\gtrless}} 0 \tag{21}$$

where

$$f(t_1) = \ln \frac{(1-\epsilon)e^{t_1} + \epsilon}{\epsilon e^{t_1} + 1 - \epsilon} \tag{22}$$

$$t_1 = \frac{q_1}{N_0}, \quad q_1 = y_d^*(n-1)y_d(n) + y_d(n-1)y_d^*(n) \tag{23}$$

$$t_0 = \frac{q_0}{N_0}, \quad q_0 = x_d^*(n-1)x_d(n) + x_d(n-1)x_d^*(n). \tag{24}$$

The nonlinear function $f(t_1)$ effectively "clips" large inputs to $\pm \ln[(1 - \epsilon)/\epsilon]$ and is approximately linear in between [6]. In particular, it was shown there that $f(t_1)$ can be approximated by a piecewise-linear (PL) function

$$f(t_1) \approx f_{PL}(t_1) \triangleq \begin{cases} -T_1, & t_1 \leq -T_1 \\ t_1, & -T_1 \leq t_1 \leq T_1 \\ T_1, & t_1 \geq T_1 \end{cases} \tag{25}$$

where $T_1 = \ln[(1 - \epsilon)/\epsilon]$ assuming $\epsilon < 0.5$. This leads to the following *PL detector*:

$$f_{PL}(t_1) + t_0 \underset{-1}{\overset{1}{\gtrless}} 0 \tag{26}$$

which is easier to implement than the ML detector (22). The PL detector achieves similar performance to that of the ML detector (see Section V) and admits tractable analysis (see Section IV).

IV. PERFORMANCE ANALYSIS

A. Average BER of DAF

Let $\gamma_{s,r,d}$ denote the equivalent instantaneous SNR of the relay link (S−R−D), which is given by [see (8)–(10)]

$$\gamma_{s,r,d} = \frac{\gamma_{s,r}\gamma_{r,d}}{\bar{\gamma}_{s,r} + 1 + \gamma_{r,d}}. \tag{27}$$

Note the above expression is different from the instantaneous SNR in [8] that uses (7) for amplification. The PDF of $\gamma_{s,r,d}$ is derived in Appendix I

$$p_{\gamma_{s,r,d}}(\gamma) = \frac{\beta^2}{2} \exp\left(-\frac{\gamma}{\bar{\gamma}_{s,r}}\right) K_0(\beta\sqrt{\gamma})$$

$$+ \frac{2}{\bar{\gamma}_{s,r}\bar{\gamma}_{r,d}} \sqrt{\frac{\gamma(1 + \bar{\gamma}_{s,r})\bar{\gamma}_{r,d}}{\bar{\gamma}_{s,r}}} \exp\left(-\frac{\gamma}{\bar{\gamma}_{s,r}}\right) K_1(\beta\sqrt{\gamma}) \tag{28}$$

where $\beta \triangleq 2\sqrt{(1 + \bar{\gamma}_{s,r})/(\bar{\gamma}_{s,r}\bar{\gamma}_{r,d})}$, $K_0(\cdot)$ denotes the zeroth-order modified Bessel function of the second kind, and $K_1(\cdot)$

denotes the first-order modified Bessel function of the second kind.

As a by product, we first determine the average BER of using only the signal received via the relay link. Although this is not the main interest of this paper, the result will be useful when source S cannot reach destination D directly due to power limitation. In this case, the average BER is given by

$$\bar{P}_{e1} = \int_0^\infty \frac{1}{2} e^{-\gamma} p_{\gamma_{s,r,d}}(\gamma) d\gamma. \tag{29}$$

After changing the variable $\sqrt{\gamma} = u$ and some algebraic manipulations, we have with the aid of [14, (6.631.3)]

$$\bar{P}_{e1} = \frac{1}{2\sqrt{\bar{\gamma}_{r,d}}} \exp\left(\frac{1}{2\bar{\gamma}_{r,d}}\right) W_{-0.5,0}\left(\frac{1}{\bar{\gamma}_{r,d}}\right)$$

$$+ \frac{1}{2(1 + \bar{\gamma}_{s,r})} \exp\left(\frac{1}{2\bar{\gamma}_{r,d}}\right) W_{-1,0.5}\left(\frac{1}{\bar{\gamma}_{r,d}}\right) \tag{30}$$

where $W_{\lambda,\mu}(\cdot)$ is the Whittaker function.

Exact performance analysis of the differential detector (14) is involved. Computer simulation suggests that the two detectors (13) and (14) have similar BER performance. An analysis of (14) is provided next. The conditional BER of differential BPSK using two independent channels is given by [13, (12.1-13)]

$$P_e(\gamma_b) = \frac{1}{8}(4 + \gamma_b)e^{-\gamma_b} \tag{31}$$

where γ_b denotes the sum of the SNR of the relay link (S−R−D) and of the direct link (S−D)

$$\gamma_b = \gamma_{s,r,d} + \gamma_{s,d}. \tag{32}$$

Averaging the conditional BER with respect to the PDF of $\gamma_{s,r,d}$ and $\gamma_{s,d}$, we have (see [14, (6.631.3)])

$$\bar{P}_e = \int_0^\infty \int_0^\infty \frac{1}{8}(4 + \gamma_1 + \gamma_2)e^{-\gamma_1 - \gamma_2}$$

$$\times p_{\gamma_{s,r,d}}(\gamma_1) p_{\gamma_{s,d}}(\gamma_2) d\gamma_1 d\gamma_2$$

$$= \exp\left(\frac{1}{2\bar{\gamma}_{r,d}}\right)$$

$$\times \left[\frac{4 + 5\bar{\gamma}_{s,d}}{8(1 + \bar{\gamma}_{s,d})^2\sqrt{\bar{\gamma}_{r,d}}} W_{-0.5,0}\left(\frac{1}{\bar{\gamma}_{r,d}}\right) \right.$$

$$+ \frac{4 + 5\bar{\gamma}_{s,d}}{8(1 + \bar{\gamma}_{s,d})^2(1 + \bar{\gamma}_{s,r})} W_{-1,0.5}\left(\frac{1}{\bar{\gamma}_{r,d}}\right)$$

$$+ \frac{\bar{\gamma}_{s,r}}{8(1 + \bar{\gamma}_{s,d})(1 + \bar{\gamma}_{s,r})\sqrt{\bar{\gamma}_{r,d}}} W_{-1.5,0}\left(\frac{1}{\bar{\gamma}_{r,d}}\right)$$

$$\left. + \frac{\bar{\gamma}_{s,r}}{4(1 + \bar{\gamma}_{s,d})(1 + \bar{\gamma}_{s,r})^2} W_{-2,0.5}\left(\frac{1}{\bar{\gamma}_{r,d}}\right) \right]. \tag{33}$$

B. Outage Probability of DAF

An outage is an event when the instantaneous SNR drops below a predetermined SNR threshold (see, e.g., [15]). The outage probability for DAF can be defined as

$$P_{\text{out}} = \int_0^{\gamma_{\text{th}}} p_{\gamma_b}(\gamma) d\gamma \tag{34}$$

where γ_{th} is a predetermined SNR threshold. We note that γ_b is the sum of two independent random variables [cf. (32)]. Hence, the PDF of γ_b is the convolution of the PDFs of $\gamma_{s,r,d}$ and $\gamma_{s,d}$ (e.g., [16])

$$p_{\gamma_b}(\gamma) = \int_0^{\gamma} p_{\gamma_{s,d}}(\gamma - \zeta) p_{\gamma_{s,r,d}}(\zeta) d\zeta$$

$$= \frac{1}{\bar{\gamma}_{s,d}} e^{-\frac{\gamma}{\bar{\gamma}_{s,d}}} \left[\beta^2 \int_0^{\sqrt{\gamma}} u e^{-\alpha u^2} K_0(\beta u) du \right.$$

$$+ \frac{4}{\bar{\gamma}_{s,r} \bar{\gamma}_{r,d}} \sqrt{\frac{(1 + \bar{\gamma}_{s,r}) \bar{\gamma}_{r,d}}{\bar{\gamma}_{s,r}}}$$

$$\left. \times \int_0^{\sqrt{\gamma}} u^2 e^{-\alpha u^2} K_1(\beta u) du \right] \quad (35)$$

where $\alpha \triangleq ((\bar{\gamma}_{s,d} - \bar{\gamma}_{s,r})/(\bar{\gamma}_{s,d} \bar{\gamma}_{s,r}))$, and we changed the variable $u \triangleq \sqrt{\zeta}$. Further simplification of (35) is difficult. However, for the symmetric case of $\bar{\gamma}_{s,r} = \bar{\gamma}_{s,d}$, (35) can be simplified and has a closed-form expression [14, (6.561.8)]

$$p_{\gamma_b}(\gamma) = \frac{1}{\bar{\gamma}_{s,d}} e^{-\frac{\gamma}{\bar{\gamma}_{s,d}}} \left[\frac{1 + \bar{\gamma}_{s,r} + \bar{\gamma}_{r,d}}{1 + \bar{\gamma}_{s,r}} \right.$$

$$\left. - \beta \sqrt{\gamma} K_1(\beta \sqrt{\gamma}) - \frac{2\gamma}{\bar{\gamma}_{s,r}} K_2(\beta \sqrt{\gamma}) \right]. \quad (36)$$

Equation (34) can be evaluated using numerical integration methods.

C. Average BER of DDF

BER analysis of the ML detector (21) is prohibitively complex due to its nonlinear nature. Instead, we derive the average BER of the PL detector (26) which not only is simpler to implement but also closely matches the performance of the ML detector. DDF is difficult to analyze partly because of decision errors made by relay R. Such relay-induced errors lead to a mixture distribution of the received signal [cf. (19)]. The analysis is further complicated by a decision statistic that involves quadratic forms in Gaussian and Gaussian mixture variates [see (23)–(24)]. Closed-form expressions of the distributions of such quadratic forms, in general, are known only via series expansion [17].

We can assume without loss of generality that $d(n) = 1$ is transmitted from source S. The error events of the PL detector can be represented using three mutually exclusive ones. Specifically, the conditional BER (conditioned on the channels) of the PL detector is

$$P_e(\gamma_{s,d}, \gamma_{r,d})$$
$$= \Pr \{t_0 - T_1 < 0 | t_1 < -T_1, d(n) = 1\}$$
$$\times \Pr \{t_1 < -T_1 | d(n) = 1\}$$
$$+ \Pr \{t_0 + T_1 < 0 | t_1 > T_1, d(n) = 1\}$$
$$\times \Pr \{t_1 > T_1 | d(n) = 1\}$$
$$+ \Pr \{t_0 + t_1 < 0, -T_1 \le t_1 \le T_1 | d(n) = 1\}. \quad (37)$$

In Appendix II, we show that the conditional BER can be written as

$$P_e(\gamma_{s,d}, \gamma_{r,d}) = (P_{e1} P_{e2} + P_{e3} P_{e4} + P_{e7})(1 - \epsilon)$$
$$+ (P_{e1} P_{e3} + P_{e2} P_{e4} + P_{e8}) \epsilon \quad (38)$$

where

$$P_{e1}(\gamma_{s,d}) = 1 - \frac{e^{-2\gamma_{s,d}}}{2}$$
$$\times \sum_{k=0}^{\infty} \sum_{n=0}^{k} \frac{2^{k-n} \gamma_{s,d}^k}{k!(k-n)!} \Gamma(k+1-n, T_1) \quad (39)$$

$$P_{e2}(\gamma_{r,d}) = \frac{e^{-\gamma_{r,d} - T_1}}{2} \quad (40)$$

$$P_{e3}(\gamma_{r,d}) = \frac{e^{-2\gamma_{r,d}}}{2}$$
$$\times \sum_{k=0}^{\infty} \sum_{n=0}^{k} \frac{2^{k-n} \gamma_{r,d}^k}{k!(k-n)!} \Gamma(k+1-n, T_1) \quad (41)$$

$$P_{e4}(\gamma_{s,d}) = \frac{e^{-\gamma_{s,d} - T_1}}{2} \quad (42)$$

$$P_{e7}(\gamma_{s,d}, \gamma_{r,d}) = \frac{1}{2} e^{-\gamma_{r,d}} - \frac{1}{2} e^{-\gamma_{r,d} - T_1} - \frac{e^{-2\gamma_{s,d} - \gamma_{r,d}}}{4}$$
$$\times \sum_{k=0}^{\infty} \sum_{n=0}^{k} \sum_{m=0}^{k-n} \frac{2^{k-n-m-1} \gamma_{s,d}^k}{k!m!} \gamma(m+1, 2T_1)$$
$$+ \frac{e^{-\gamma_{s,d} - 2\gamma_{r,d}}}{8}$$
$$\times \sum_{k=0}^{\infty} \sum_{n=0}^{k} \frac{\gamma_{r,d}^k}{k!(k-n)!} \gamma(k-n+1, 2T_1) \quad (43)$$

$$P_{e8}(\gamma_{s,d}, \gamma_{r,d}) = \frac{e^{-2\gamma_{r,d}}}{2} \sum_{k=0}^{\infty} \sum_{n=0}^{k} \frac{2^{k-n} \gamma_{r,d}^k}{k!(k-n)!} \gamma(k-n+1, T_1)$$
$$- \frac{e^{-2\gamma_{s,d} - 2\gamma_{r,d}}}{8}$$
$$\times \sum_{k=0}^{\infty} \sum_{i=0}^{\infty} \sum_{n=0}^{k} \sum_{j=0}^{i} \sum_{m=0}^{i-j} \frac{\gamma_{r,d}^k \gamma_{s,d}^i}{k!(k-n)!i!m!2^{j+m-i}}$$
$$\times \gamma(k-n+m+1, 2T_1)$$
$$+ \frac{1}{8} e^{-\gamma_{s,d} - \gamma_{r,d}} (1 - e^{-2T_1}) \quad (44)$$

and the upper and lower incomplete Gamma function are defined as $\Gamma(a, x) = \int_x^{\infty} e^{-t} t^{a-1} dt$ and $\gamma(a, x) = \int_0^x e^{-t} t^{a-1} dt$, respectively. Notice that the conditional BER only depends on the instantaneous SNRs $\gamma_{r,d}$ and $\gamma_{s,d}$, and the error probability ϵ at R.

The average BER for DDF is obtained by averaging (38) using the distribution of $\gamma_{r,d}$ and $\gamma_{s,d}$

$$\bar{P}_e = \int_0^{\infty} \int_0^{\infty} P_e(\gamma_1, \gamma_2) p_{\gamma_{s,d}}(\gamma_1) p_{\gamma_{r,d}}(\gamma_2) d\gamma_1 d\gamma_2. \quad (45)$$

A close examination of (39)–(44) reveals that the 2-D integration in (45) is separable. Using [14, (3.351.3)], we arrive at the following closed-form expression of the average BER for DDF:

$$\bar{P}_e = (\bar{P}_{e1} \bar{P}_{e2} + \bar{P}_{e3} \bar{P}_{e4} + \bar{P}_{e7})(1 - \epsilon) + (\bar{P}_{e1} \bar{P}_{e3} + \bar{P}_{e2} \bar{P}_{e4} + \bar{P}_{e8}) \epsilon \quad (46)$$

where

$$\bar{P}_{e1} = 1 - \frac{1}{2(2\bar{\gamma}_{s,d}+1)}$$
$$\times \sum_{k=0}^{\infty} \sum_{n=0}^{k} \frac{2^{k-n}\bar{\gamma}_{s,d}^k \Gamma(k+1-n,T_1)}{(k-n)!(2\bar{\gamma}_{s,d}+1)^k} \quad (47)$$

$$\bar{P}_{e2} = \frac{1}{2(\bar{\gamma}_{r,d}+1)} e^{-T_1} \quad (48)$$

$$\bar{P}_{e3} = \frac{1}{2(2\bar{\gamma}_{r,d}+1)} \sum_{k=0}^{\infty} \sum_{n=0}^{k} \frac{2^{k-n}\bar{\gamma}_{r,d}^k \Gamma(k+1-n,T_1)}{(k-n)!(2\bar{\gamma}_{r,d}+1)^k} \quad (49)$$

$$\bar{P}_{e4} = \frac{1}{2(\bar{\gamma}_{s,d}+1)} e^{-T_1} \quad (50)$$

$$\bar{P}_{e7} = \frac{1}{2(\bar{\gamma}_{r,d}+1)}(1 - e^{-T_1}) - \frac{1}{8(2\bar{\gamma}_{s,d}+1)(\bar{\gamma}_{r,d}+1)}$$
$$\times \sum_{k=0}^{\infty} \sum_{n=0}^{k} \sum_{m=0}^{k-n} \frac{2^{k-n-m}\bar{\gamma}_{s,d}^k \gamma(m+1,2T_1)}{m!(2\bar{\gamma}_{s,d}+1)^k}$$
$$\times \frac{1}{8(\bar{\gamma}_{s,d}+1)(2\bar{\gamma}_{r,d}+1)}$$
$$\times \sum_{k=0}^{\infty} \sum_{n=0}^{k} \frac{\bar{\gamma}_{r,d}^k \gamma(k+1-n,2T_1)}{(k-n)!(2\bar{\gamma}_{r,d}+1)^k} \quad (51)$$

[see (52), shown at the bottom of the page].

D. Alternative Average BER of DDF: Approximation

Since convergence rate could be slow with a series expansion approach, we provide next an alternative BER expression for the DDF scheme by approximations valid in the high SNR regime. However, it is shown in Section V that the approximate BER obtained here is very close to the exact BER over a wide range of SNR of practical interest.

First, note that t_0 in (24) is a quadratic form of Gaussian variates $x_d(n-1)$ and $x_d(n)$. At the high SNR regime, we may ignore the cross term of the Gaussian noise components of $x_d(n-1)$ and $x_d(n)$ (see [13, p. 273] for details) and approximate the conditional distribution of t_0 as $\mathcal{N}(2\gamma_{s,d}d(n),4\gamma_{s,d})$, where $\mathcal{N}(\mu,\sigma^2)$ denotes a real Gaussian random variable with mean μ and variance σ^2. Likewise, t_1 in (23) is a quadratic form of Gaussian mixture variate $y_d(n-1)$ and $y_d(n)$. At high SNR, we can ignore the cross noise term in t_1 and approximate its distribution as a Gaussian mixture

$$p_{t_1}(y) \approx (1-\epsilon)\Phi(y;2\gamma_{r,d}d(n),4\gamma_{r,d})$$
$$+\epsilon\Phi(y;-2\gamma_{r,d}d(n),4\gamma_{r,d}) \quad (53)$$

where $\Phi(q;\mu,\sigma^2)$ denotes the PDF of a real Gaussian random variable with mean μ and variance σ^2. Based on the above approximations, the conditional BER (37) can be expressed as

$$P_e(\gamma_{s,d},\gamma_{r,d})$$
$$\approx Q\left(\frac{2\gamma_{s,d}-T_1}{2\sqrt{\gamma_{s,d}}}\right)$$
$$\times \left[(1-\epsilon)Q\left(\frac{2\gamma_{r,d}+T_1}{2\sqrt{\gamma_{r,d}}}\right) + \epsilon Q\left(\frac{T_1-2\gamma_{r,d}}{2\sqrt{\gamma_{r,d}}}\right)\right]$$
$$+ Q\left(\frac{T_1+2\gamma_{s,d}}{2\sqrt{\gamma_{s,d}}}\right)$$
$$\times \left[(1-\epsilon)Q\left(\frac{T_1-2\gamma_{r,d}}{2\sqrt{\gamma_{r,d}}}\right) + \epsilon Q\left(\frac{T_1+2\gamma_{r,d}}{2\sqrt{\gamma_{r,d}}}\right)\right]$$
$$+ \int_{-T_1}^{T_1} dy p_{t_1}(y)Q\left(\frac{2\gamma_{s,d}+y}{2\sqrt{\gamma_{s,d}}}\right) \quad (54)$$

where $Q(\cdot)$ denotes the standard Gaussian Q function. Averaging the conditional BER across channel statistics yields the approximate average BER, which has the same form of (45).

A discussion on the computational aspect of the results in this and previous section follows. The integrals in (54) and (45) can be computed using standard numerical integration techniques, such as the Gaussian quadrature method [18]. On the other hand, the infinite series in (48)–(52) are truncated to a finite number of terms for practical implementation. The upper and lower incomplete Gamma functions used there can be calculated by

$$\Gamma(n,x) = (n-1)!e^{-x}\sum_{m=0}^{n-1} x^m/m! \quad (55)$$

$$\gamma(n,x) = (n-1)! - \Gamma(n,x). \quad (56)$$

As an example of comparison, we consider the case of truncating the infinite series to 600 terms, and it takes about 614 s of CPU time measured by Matlab on a 3-GHz Pentium PC to get the average BER using (46)–(52). Meanwhile, using (54) and (45) with the Gaussian quadrature method takes only 19 s, which yields a numerically identical BER result and is significantly more efficient. These numbers are only for illustration purpose, and our Matlab codes are not streamlined to achieve the best computational efficiency. The complexity of using (46)–(52) is reduced by keeping fewer terms after truncation, but this may affect the accuracy of the result, especially at high SNR.

E. Outage Probability of DDF

For DDF, we cannot employ a single instantaneous SNR at destination D as an indicator of outage due to decision errors at relay R. In fact, the outage for decode-based schemes (including

$$\bar{P}_{e8} = \frac{1}{2(2\bar{\gamma}_{r,d}+1)} \sum_{k=0}^{\infty} \sum_{n=0}^{k} \frac{2^{k-n}\bar{\gamma}_{r,d}^k \gamma(k+1-n,T_1)}{(k-n)!(2\bar{\gamma}_{r,d}+1)^k} - \frac{1}{8(2\bar{\gamma}_{s,d}+1)(2\bar{\gamma}_{r,d}+1)}$$
$$\times \sum_{k=0}^{\infty} \sum_{i=0}^{\infty} \sum_{n=0}^{k} \sum_{j=0}^{i} \sum_{m=0}^{i-j} \frac{\bar{\gamma}_{r,d}^k (2\bar{\gamma}_{s,d})^i \gamma(k+m+1-n,2T_1)}{(2\bar{\gamma}_{r,d}+1)^k(2\bar{\gamma}_{s,d}+1)^i(k-n)!m!2^{j+m}} + \frac{1}{8(\bar{\gamma}_{s,d}+1)(\bar{\gamma}_{r,d}+1)}(1-e^{-2T_1}) \quad (52)$$

DDF) is not unanimously established. From an information-theoretic perspective, outage capacity is used in [5], which is suitable for coded DF schemes. For the uncoded case, we can define that an outage of the cooperative system occurs when both the direct and relay links experience outage. A similar definition of the outage for the relay link was used in [7]. Hence, the outage probability for DDF is given by

$$P_{\text{out}} = P_{\text{out}}^{s,d} P_{\text{out}}^{s,r,d} \qquad (57)$$

where $P_{\text{out}}^{s,d}$ and $P_{\text{out}}^{s,r,d}$ denote the outage probability of the direct and relay link, respectively. Specifically, $P_{\text{out}}^{s,d}$ is the probability with which $\gamma_{s,d}$ drops below threshold γ_{th}

$$P_{\text{out}}^{s,d} \triangleq \int_{0}^{\gamma_{\text{th}}} p_{\gamma_{s,d}}(\gamma) d\gamma = 1 - e^{-\gamma_{\text{th}}/\bar{\gamma}_{s,d}} \qquad (58)$$

while $P_{\text{out}}^{s,r,d}$ is the probability with which either $\gamma_{s,r}$ or $\gamma_{r,d}$ drops below γ_{th}

$$\begin{aligned} P_{\text{out}}^{s,r,d} &\triangleq P(\gamma_{s,r} \leq \gamma_{\text{th}} \cup \gamma_{r,d} \leq \gamma_{\text{th}}) \\ &= 1 - P(\gamma_{s,r} > \gamma_{\text{th}}, \gamma_{r,d} > \gamma_{\text{th}}) \\ &= 1 - e^{-\gamma_{\text{th}}(1/\bar{\gamma}_{s,r} + 1/\bar{\gamma}_{r,d})}. \end{aligned} \qquad (59)$$

F. Asymptotic Analysis and Diversity Order

To gain additional insight into the above BER and outage analysis, we examine in this section the asymptotic performance at high SNR and diversity gain of the proposed DAF and DDF schemes.

First, consider DAF whose average BER is given by (33). To simplify our analysis, we consider the symmetric case with $\bar{\gamma}_{s,r} = \bar{\gamma}_{s,d} = \bar{\gamma}_{r,d} = \rho$ and let $\rho \to \infty$. For large ρ, (33) can be approximated as

$$\begin{aligned} \bar{P}_e \approx \frac{1}{8} \rho^{-2} &\left[5U(1,1,\rho^{-1}) + U(2,1,\rho^{-1}) \right. \\ &\left. + 5\rho^{-1}U(2,2,\rho^{-1}) + 2\rho^{-1}U(3,2,\rho^{-1}) \right] \end{aligned} \qquad (60)$$

where we used the result [19, (13.1.33)]

$$W_{\lambda,\mu}(z) = e^{-z/2} z^{\mu+1/2} U(1/2 + \mu - \lambda, 1 + 2\mu, z) \qquad (61)$$

and $U(a, b, z)$ is the confluent hypergeometric function of the second kind. $U(1, 1, \rho^{-1})$ and $U(2, 1, \rho^{-1})$ behave like $\ln(\rho^{-1})$ for large ρ [19, (13.5.7)], while $U(2, 2, \rho^{-1})$ and $U(3, 2, \rho^{-1})$ behave like ρ for large ρ [19, (3.5.9)]. Using these facts in (60) yields

$$\bar{P}_e \propto C_{\text{DAF}} \rho^{-2} \ln \rho, \quad \text{for large } \rho \qquad (62)$$

where C_{DAF} is a constant. Noting that $\lim_{\rho \to \infty} \rho^{-\epsilon} \ln \rho = 0$, $\forall \epsilon > 0$, we conclude that the diversity gain of the DAF is 2 as $\rho \to \infty$.

Next, we consider the DDF scheme. Although we may find the diversity gain from the average BER in (45) or (46) by letting the SNR approach infinity, this turns out a tedious process.

Instead, we will use the outage probability to determine its diversity gain. It has been shown that using either the outage probability or average BER leads to identical results pertaining to the diversity gain of a wireless communication system [20]. Again, we consider the symmetric case with $\bar{\gamma}_{s,r} = \bar{\gamma}_{s,d} = \bar{\gamma}_{r,d} = \rho$ and let $\rho \to \infty$. A second-order Taylor expansion of (58) and (59), followed by a substitution back into (57), yields

$$P_{\text{out}} \propto C_{\text{DDF}} \gamma_{\text{th}}^2 \rho^{-2}, \quad \text{for large } \rho \qquad (63)$$

where C_{DDF} is a constant. Hence, the DDF has a diversity order of 2. Note that DDF does not have the $\ln \rho$ term in (63), which suggests that DDF may enjoy a steeper slope than DAF for finite ρ.

V. NUMERICAL RESULTS

We consider the cooperative wireless system shown in Fig. 1 with Rayleigh fading channels, and verify our analytical results with simulation. Unless specified otherwise, we consider a *symmetric* scenario where the average SNRs of all hops are identical: $\bar{\gamma}_{s,d} = \bar{\gamma}_{s,r} = \bar{\gamma}_{r,d}$. We compare our cooperative system to a conventional noncooperative system that involves direct transmission from S to D with differential BPSK (DBPSK). For fair comparison, we set $\bar{\gamma}_{s,d} = \bar{\gamma}_{s,r} = \bar{\gamma}_{r,d} = 0.5E_b/N_0$, so that the sum of the transmitted energy from both S and R for the cooperative system is identical to that of the noncooperative system.

Fig. 2 shows the average BER of DAF using either (13) or (14), the average BER of DDF with ML (21) or PL (26) detection (dubbed as *DDF-ML* and *DDF-PL*, respectively), and the average BER of the noncooperative differential BPSK (20). We first note that in the current case, using (13) or (14) yields nearly identical simulation results, which also match the analytical results obtained in (33). For the analytical results regarding the average BER of DDF-PL, both the exact expression and the approximate expression are shown in Fig. 2, where we see that they are visually identical over all SNRs under consideration. Overall, it is seen that our analytical results are matched by the simulation results. DDF-PL is only slightly worse than DDF-ML, and our cooperative schemes achieve cooperative diversity and outperform the noncooperative DBPSK. For comparison, we also plot in Fig. 2 the average BERs of AF and DF schemes applying coherent detection (with perfect CSI). It is observed that the coherent AF outperforms DAF by about 5 dB at BER 10^{-4}; DDF-ML and DDF-PL incur a SNR penalty of about 1.7 and 2 dB, respectively, compared with coherent DF-PL scheme at BER 10^{-4}.

For *asymmetric* setups, (13) and (14) are still found to yield similar BER performance as long as the per-hop average SNRs are not significantly different. We next consider a more asymmetric case with $\bar{\gamma}_{s,d} = \bar{\gamma}_{s,r} = (1/11)E_b/N_0$, and $\bar{\gamma}_{r,d} = (10/11)E_b/N_0$. That is, $\bar{\gamma}_{r,d}$ is 10 dB stronger than $\bar{\gamma}_{r,d}$ and $\bar{\gamma}_{s,r}$. This also corresponds to the case where R is close to D, but both are far away from S. In addition to the *unequal gain combiners* (13) and (14), we also consider the standard equal gain combiner (EGC), which instead uses the following $z(n)$:

$$z(n) = x_d^*(n-1)x_d(n) + y_d^*(n-1)y_d(n). \qquad (64)$$
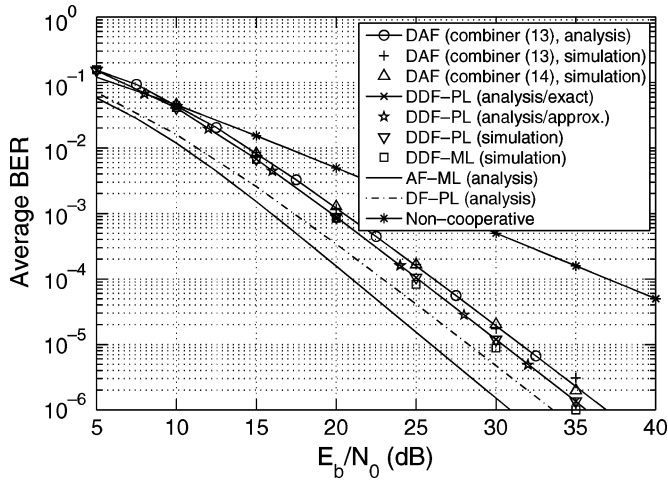
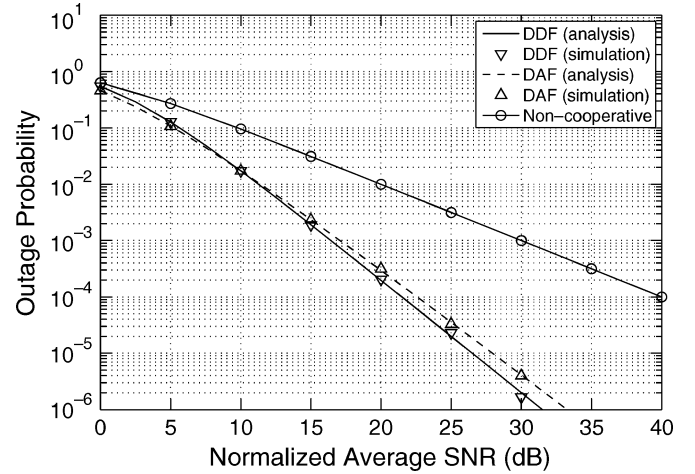Fig. 2. Average BER in Rayleigh fading channels.

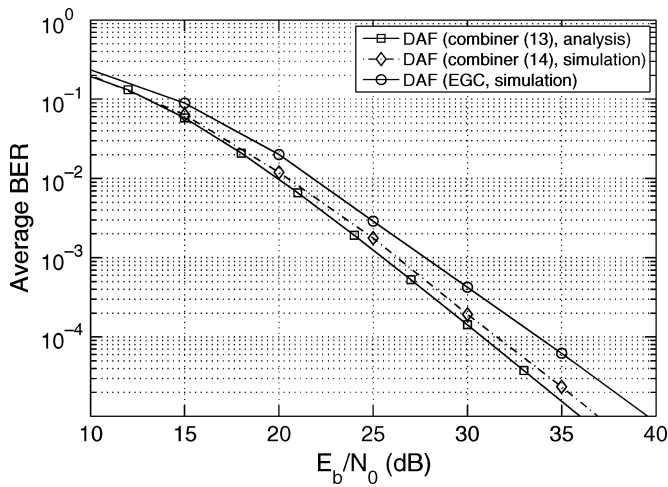Fig. 4. Outage probability in Rayleigh fading channels.
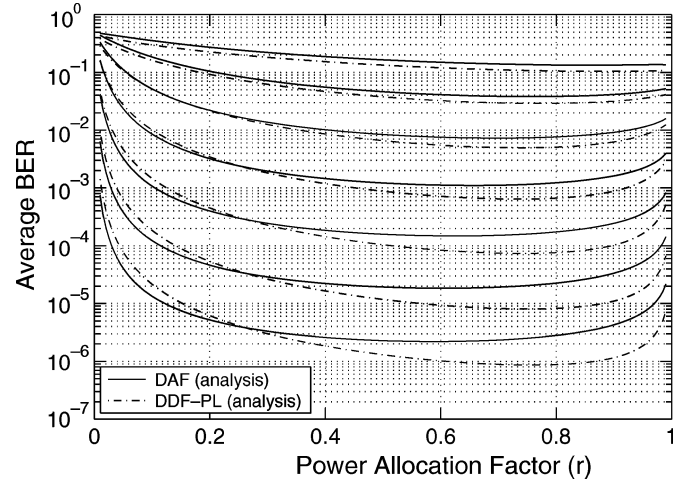

Fig. 3. Comparison of different combiners for DAF in an *asymmetric* scenario.

Fig. 5. Average BER of the DAF and DDF schemes as a function of the power allocation factor r for $E_b/N_0 = 5, 10, \ldots, 35$ dB (SNR increases from top to bottom) in Rayleigh fading channels.

The average BERs of the three combiners are shown in Fig. 3. It is seen that (14) is about 0.7 dB worse than the clairvoyant combiner (13) at BER 10^{-4}, but outperforms the EGC by more than 2 dB. Hence, it is beneficial to use our unequal gain combiner (14) which takes into account the unequal average SNRs of the direct link and relay link. We reiterate that the clairvoyant combiner (13) requires CSI and is not suitable for differential demodulation.

Fig. 4 illustrates the outage probabilities for the proposed and the noncooperative schemes, where we let $\bar{\gamma}_{s,d} = \bar{\gamma}_{s,r} = \bar{\gamma}_{r,d} = 0.5 E_b/N_0$, and the threshold $\gamma_{\text{th}} = 10$ dB. The horizontal axis in Fig. 4 is the average SNR normalized by γ_{th}. DAF and DDF are again seen to yield diversity gain over the noncooperative scheme. It is also seen that DDF has a slightly steeper slope than DAF, confirming the earlier conjecture.

Assuming equal distance between S, R, and D, the symmetric case considered in Figs. 2 and 4 corresponds to allocating *equal power* to S and R. To examine the impact of different power allocation schemes, we introduce a *power allocation factor* $0 < r < 1$ that controls power allocation as follows: $\bar{\gamma}_{s,r} = \bar{\gamma}_{s,d} = r E_b/N_0$ and $\bar{\gamma}_{r,d} = (1 - r)E_b/N_0$. In effect, $r > 0.5$ means

more power allocated to S than to R, and vice versa. Fig. 5 depicts the average BER of DAF and DDF-PL as a function of r (horizontal axis) for $E_b/N_0 = 5, 10, \ldots, 35$ dB. For the range of SNRs in Fig. 5, DAF appears to favor equal power allocation ($r = 0.5$), while DDF seems to yield the lowest BER when $r \approx 0.75$, *viz.*, when the power allocated to S is approximately three times that allocated to R.

Consider a different scenario in which S and R are provided with identical transmission power, but the inter-node distance between S, R, and D are different. The question now becomes where we shall place R to achieve the best performance. Our observation in Fig. 5 implies that for DAF to yield the best performance, R shall be approximately located in the mid-point between S and D. This observation, along with those in [9] and [10], suggests that the optimal position of relay may be independent of specific modulation scheme for AF based strategies. Meanwhile for DDF, R shall be closer to S than to D. The result pertaining to DDF is intuitive since as R is further away from S, the former is expected to incur more decision errors, making the relay link increasingly less useful.
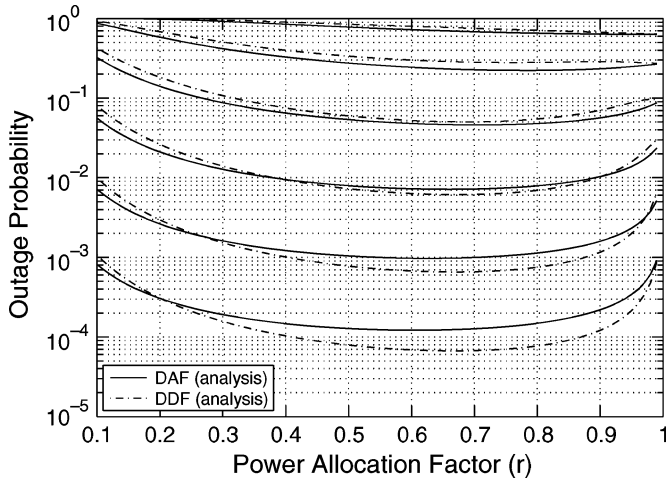
Fig. 6. Outage probability of the DAF and DDF schemes as a function of the power allocation factor r for $E_b/N_0 = 10, 15, \ldots, 35$ dB (SNR increases from top to bottom) in Rayleigh fading channels.

Fig. 6 depicts the outage probability versus the power allocation factor for DAF and DDF. We set the threshold $\gamma_{th} = 10$ dB, and $E_b/N_0 = 10, 15, \ldots, 35$ dB. The same pattern is observed as in Fig. 5.

VI. CONCLUSION

We have examined two binary differential modulation schemes, namely DAF and DDF, along with their corresponding combining/detection techniques, for cooperative wireless networks. We have presented a framework of analytical results for the DAF and DDF schemes, including the PDF of the instantaneous SNR, average BER, and outage probability in Rayleigh fading channels. These results attest that DAF and DDF achieve cooperative diversity and outperform conventional noncooperative techniques.

APPENDIX I
PDF OF $\gamma_{s,r,d}$

Let $X = \gamma_{s,r}\gamma_{r,d}$ and $Y = \bar{\gamma}_{s,r} + \gamma_{r,d} + 1$. The PDF of $\gamma_{s,r,d}$ is determined as follows (e.g., [16]):

$$
\begin{aligned}
&p_{\gamma_{s,r,d}}(\gamma) \\
&= \int_{\bar{\gamma}_{s,r}+1}^{\infty} |y| p_{X,Y}(\gamma y, y) dy \\
&= \int_{0}^{\infty} |\bar{\gamma}_{s,r} + 1 + \gamma_{r,d}| \\
&\quad \times p_{X,Y}\left(\gamma(\bar{\gamma}_{s,r} + 1 + \gamma_{r,d}), (\bar{\gamma}_{s,r} + 1 + \gamma_{r,d})\right) d\gamma_{r,d}
\end{aligned}
\tag{65}
$$

where $p_{X,Y}(x,y) = p_{X|Y}(x|y)p_Y(y)$ denotes the joint PDF of X and Y. The marginal PDF of Y is given by

$$
p_Y(y) = \frac{1}{\bar{\gamma}_{r,d}} e^{-\frac{y-\bar{\gamma}_{s,r}-1}{\bar{\gamma}_{r,d}}}.
\tag{66}
$$

The conditional PDF of $p_{X|Y}(x|y)$ is given by

$$
p_{X|Y}(x|y) = \frac{1}{\bar{\gamma}_{s,r}|y - \bar{\gamma}_{s,r} - 1|} e^{-\frac{x}{\bar{\gamma}_{s,r}(y-\bar{\gamma}_{s,r}-1)}}.
\tag{67}
$$

Substituting (66) and (67) into (65), after some manipulations, we have

$$
\begin{aligned}
p_{\gamma_{s,r,d}}(\gamma) &= \frac{\bar{\gamma}_{s,r}+1}{\bar{\gamma}_{s,r}\bar{\gamma}_{r,d}} e^{-\frac{\gamma}{\bar{\gamma}_{s,r}}} \int_{0}^{\infty} \frac{1}{\gamma_{r,d}} e^{-a\gamma_{r,d}-b\gamma_{r,d}^{-1}} d\gamma_{r,d} \\
&\quad + \frac{1}{\bar{\gamma}_{s,r}\bar{\gamma}_{r,d}} e^{-\frac{\gamma}{\bar{\gamma}_{s,r}}} \int_{0}^{\infty} e^{-a\gamma_{r,d}-b\gamma_{r,d}^{-1}} d\gamma_{r,d}
\end{aligned}
\tag{68}
$$

where $a = 1/\bar{\gamma}_{r,d}$, $b = \gamma_{s,r,d}(1 + \bar{\gamma}_{s,r})/\bar{\gamma}_{s,r}$. With the aid of [14, (3.478.4)], (68) can be written as (28).

APPENDIX II
CONDITIONAL BER FOR PL DETECTOR

The decision statistics t_0 and t_1 in (37) are quadratic forms [cf. (23)–(24)] of Gaussian and, respectively, Gaussian mixture variates. To carry out the calculation in (37), we need distributions of these quadratic forms. Quadratic forms in Gaussian variates have been extensively studied (e.g., [17] and references therein). Generally, closed-form expressions of the distributions of quadratic forms in Gaussian variates exist only in series expansion. In the sequel, we will employ the series expansion results in [21] pertaining to distributions of indefinite quadratic forms in complex Gaussian variables. Although distributions of general quadratic forms in Gaussian mixture variables are not available, the q_1 related events in (37) can be dealt with by conditioning on possible decisions made at the relay, which reduces the problem to one involving only quadratic forms of Gaussian variates. This will become clear shortly.

Since t_0 and t_1 are mutually independent, we have

$$
\begin{aligned}
P_{e1}(\gamma_{s,d}) &\triangleq \Pr\{t_0 - T_1 < 0 | t_1 < -T_1, d(n) = 1\} \\
&= \Pr\{q_0 - N_0 T_1 < 0 | d(n) = 1\}
\end{aligned}
\tag{69}
$$

$$
\begin{aligned}
P_{e4}(\gamma_{s,d}) &\triangleq \Pr\{t_0 + T_1 < 0 | t_1 > T_1, d(n) = 1\} \\
&= \Pr\{q_0 + N_0 T_1 < 0 | d(n) = 1\}.
\end{aligned}
\tag{70}
$$

Applying the results regarding distributions of quadratic forms in Gaussian variates in [21], we can verify that the conditional cumulative distribution function (CDF) of q_0, conditioned on $d(n) = 1$ and the channels, is given by [see (24)]

$$
F_{q_0}(x) = \begin{cases} 1 - \frac{e^{-2\gamma_{s,d}}}{2} \\ \quad \times \sum_{k=0}^{\infty} \sum_{n=0}^{k} \frac{(2\gamma_{s,d})^k}{k!} \frac{\Gamma(k+1-n, x/N_0)}{(k-n)! 2^n}, & x > 0 \\ \frac{1}{2} e^{-\gamma_{s,d}+x/N_0} & x \leq 0. \end{cases}
\tag{71}
$$

Equations (39) and (42) follow immediately from (71).

For the probabilities related to t_1, the error events can be grouped into two mutually exclusive subevents: one corresponding to when an error is made at the relay, and one otherwise. Therefore

$$\Pr\{t_1 < -T_1 | d(n) = 1\}$$
$$= (1 - \epsilon)P_{e2}(\gamma_{r,d}) + \epsilon P_{e3}(\gamma_{r,d}) \quad (72)$$
$$\Pr\{t_1 > T_1 | d(n) = 1\}$$
$$= (1 - \epsilon)P_{e5}(\gamma_{r,d}) + \epsilon P_{e6}(\gamma_{r,d}) \quad (73)$$

where

$$P_{e2}(\gamma_{r,d}) \triangleq \Pr\left\{t_1 < -T_1 | d(n) = 1, \tilde{d}(n) = 1\right\} \quad (74)$$

$$P_{e3}(\gamma_{r,d}) \triangleq \Pr\left\{t_1 < -T_1 | d(n) = 1, \tilde{d}(n) = -1\right\} \quad (75)$$

$$P_{e5}(\gamma_{r,d}) \triangleq \Pr\left\{t_1 > T_1 | d(n) = 1, \tilde{d}(n) = 1\right\} \quad (76)$$

$$P_{e6}(\gamma_{r,d}) \triangleq \Pr\left\{t_1 > T_1 | d(n) = 1, \tilde{d}(n) = -1\right\}. \quad (77)$$

Note that conditioned on $\tilde{d}(n)$, t_1 becomes a quadratic form in Gaussian random variates. Hence, the distribution results in [21] are applicable. Following the same steps that were used to obtain (39) and (42), we get (40) and (41). Note that we have $P_{e5}(\gamma_{r,d}) = P_{e3}(\gamma_{r,d})$, and $P_{e6}(\gamma_{r,d}) = P_{e2}(\gamma_{r,d})$ because of the symmetry of the PL function $f_{PL}(t_1)$.

The last term in (37) can be written as

$$\Pr\{t_0 + t_1 < 0, -T_1 \le t_1 \le T_1 | d(n) = 1\}$$
$$= (1 - \epsilon)P_{e7}(\gamma_{s,d}, \gamma_{r,d}) + \epsilon P_{e8}(\gamma_{s,d}, \gamma_{r,d}) \quad (78)$$

where

$$P_{e7}(\gamma_{s,d}, \gamma_{r,d}) \triangleq \Pr\{t_0 + t_1 < 0, -T_1 \le t_1$$
$$\le T_1 | d(n) = 1, \tilde{d}(n) = 1\} \quad (79)$$

$$P_{e8}(\gamma_{s,d}, \gamma_{r,d}) \triangleq \Pr\{t_0 + t_1 < 0, -T_1 \le t_1$$
$$\le T_1 | d(n) = 1, \tilde{d}(n) = -1\}. \quad (80)$$

P_{e7} and P_{e8} can be found by integrating the joint PDF of q_0 and q_1, which are independent, over the constrained region

$$P_{e7}(\gamma_{s,d}, \gamma_{r,d}) = P_{e8}(\gamma_{s,d}, \gamma_{r,d})$$
$$= \int_{-N_0 T_1}^{N_0 T_1} p_{q_1}(y) dy \int_{-\infty}^{-y} p_{q_0}(x) dx$$
$$= \int_{-N_0 T_1}^{0} p_{q_1}(y) F_{q_0}(-y) dy$$
$$+ \int_{0}^{N_0 T_1} p_{q_1}(y) F_{q_0}(-y) dy. \quad (81)$$

Given $\tilde{d}(n) = 1$, q_1 is a quadratic form in Gaussian variates and its conditional PDF (conditioned on $d(n) = \tilde{d}(n) = 1$ and channels) is obtained from [21]

$$p_{q_1}(x) = \begin{cases} \frac{1}{2N_0} e^{-\frac{x}{N_0} - 2\gamma_{r,d}} \\ \times \sum_{k=0}^{\infty} \sum_{n=0}^{k} x^{k-n} \frac{(2\gamma_{r,d})^k N_0^{n-k}}{k!(k-n)!2^n}, & x > 0 \\ \frac{1}{2N_0} e^{\frac{x}{N_0} - \gamma_{r,d}} & x \le 0. \end{cases} \quad (82)$$

Substituting (71) and (82) into (81), followed by some manipulations, yields (43), where we also used [14, (3.381.1)] and the fact that

$$\Gamma(n, x) = (n - 1)! e^{-x} \sum_{m=0}^{n-1} x^k / m!. \quad (83)$$

Given $d(n) = 1$, $\tilde{d}(n) = -1$ and the channels, the PDF of q_1 is given by [21]

$$p_{q_1}(x) = \begin{cases} \frac{1}{2N_0} e^{-x/N_0 - \gamma_{r,d}}, & x > 0 \\ \frac{1}{2N_0} e^{\frac{x}{N_0} - 2\gamma_{r,d}} \\ \times \sum_{k=0}^{\infty} \sum_{n=0}^{k} (-x)^{k-n} \frac{(2\gamma_{r,d})^k N_0^n}{k! N_0^k (k-n)! 2^n}, & x \le 0. \end{cases} \quad (84)$$

Substituting (71) and (84) into (81), after some manipulations and with the help of [14, (3.381.1)], we reach (44).

ACKNOWLEDGMENT

REFERENCES

[1] E. C. van der Meulen, "Three-terminal communication channels," *Adv. Appl. Probab.*, vol. 3, pp. 120–154, 1971.

[2] T. M. Cover and A. A. El Gamal, "Capacity theorem for the relay channel," *IEEE Trans. Inf. Theory*, vol. 25, no. 5, pp. 572–584, Sep. 1979.

[3] A. Sendonaris, E. Erkip, and B. Aazhang, "User cooperation diversity—Part I: System description," *IEEE Trans. Commun.*, vol. 51, no. 11, pp. 1927–1938, Nov. 2003.

[4] ——, "User cooperation diversity—Part II: Implementation aspects and performance analysis," *IEEE Trans. Commun.*, vol. 51, no. 11, pp. 1939–1948, Nov. 2003.

[5] J. N. Laneman, D. N. C. Tse, and G. W. Wornell, "Cooperative diversity in wireless networks: Efficient protocols and outage behavior," *IEEE Trans. Inf. Theory*, vol. 50, no. 12, pp. 3062–3080, Dec. 2004.

[6] J. N. Laneman and G. W. Wornell, "Energy-efficient antenna sharing and relaying for wireless networks," presented at the IEEE Wireless Communications and Networking Conf., Chicago, IL, Sep. 2000.

[7] M. O. Hasna and M. S. Alouini, "End-to-end performance of transmission systems with relays over Rayleigh-fading channels," *IEEE Trans. Wireless Commun.*, vol. 2, no. 6, pp. 1126–1131, Nov. 2003.

[8] ——, "Harmonic mean and end-to-end performance of transmission systems with relays," *IEEE Trans. Commun.*, vol. 52, no. 1, pp. 130–135, Jan. 2004.

[9] A. Ribeiro, X. Cai, and G. B. Giannakis, "Symbol error probabilities for general cooperative links," *IEEE Trans. Wireless Commun.*, vol. 4, no. 3, pp. 1264–1273, May 2005.

[10] D. Chen and J. N. Laneman, "Modulation and demodulation for cooperative diversity in wireless systems," *IEEE Trans. Wireless Commun.*, to be published.

[11] B. M. Hochwald and T. L. Marzetta, "Unitary space-time modulation for multiple-antenna communications in Rayleigh flat fading," *IEEE Trans. Inf. Theory*, vol. 46, no. 2, pp. 543–564, Mar. 2000.

[12] Q. Zhao and H. Li, "Differential BPSK modulation for wireless relay networks," presented at the 38th Annu. Conf. Information Sciences and Systems, Princeton, NJ, Mar. 2004.

[13] J. G. Proakis, *Digital Communications*, 4th ed. New York: McGraw-Hill, 2000.

[14] I. S. Gradshteyn and I. M. Ryzhik, *Table of Integrals, Series, and Products*, 6th ed. San Diego, CA: Academic, 2000.

[15] M. K. Simon and M.-S. Alouini, *Digital Communications Over Fading Channels: A Unified Approach to Performance Analysis*. New York: Wiley, 2000.

[16] A. Papoulis, *Probability, Random Variables, and Stochastic Processes*, 3rd ed. New York: McGraw-Hill, 1991.

[17] A. M. Mathai and S. B. Provost, *Quadratic Forms in Random Variables*. New York: Marcel Dekker, 1992.

[18] G. W. Recktenwald, *Numerical Methods With MATLAB: Implementations and Applications*. Upper Saddle River, NJ: Prentice Hall, 2000.

[19] M. Abramowitz and I. A. Ryzhik, *Handbook of Mathematical Functions With Formulas, Groupes, and Mathematical Tables*. New York: Dover, 1972.

[20] Z. Wang and G. B. Giannakis, "A simple and general parameterization quantifying performance in fading channels," *IEEE Trans. Commun.*, vol. 51, no. 8, pp. 1389–1398, Aug. 2003.

[21] K. H. Biyari and W. C. Lindsey, "Statistical distributions of Hermitian quadratic forms in complex Gaussian variables," *IEEE Trans. Inf. Theory*, vol. 39, no. 3, pp. 1076–1082, May 1993.
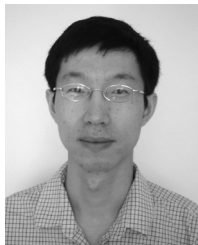
Qiang Zhao received the M.S. degree in electrical engineering from Virginia Tech, Blacksburg, VA, and the Ph.D. degree in electrical engineering from the Stevens Institute of Technology, Hoboken, NJ, in 2006.

His interests include cooperative diversity and wireless relay networks.

Hongbin Li (M'99) received the B.S. and M.S. degrees from the University of Electronic Science and Technology of China, Chengdu, in 1991 and 1994, respectively, and the Ph.D. degree from the University of Florida, Gainesville, in 1999, all in electrical engineering.

From July 1996 to May 1999, he was a Research Assistant in the Department of Electrical and Computer Engineering, University of Florida. He was a Summer Visiting Faculty Member at the Air Force Research Laboratory, Rome, NY, during the summers of 2003 and 2004. Since July 1999, he has been with the Department of Electrical and Computer Engineering, Stevens Institute of Technology, Hoboken, NJ, where he is an Associate Professor. His current research interests include wireless communications and networking, statistical signal processing, and radars.

Dr. Li is a member of Tau Beta Pi and Phi Kappa Phi. He received the Harvey N. Davis Teaching Award in 2003 and the Jess H. Davis Memorial Award for excellence in research in 2001 from the Stevens Institute of Technology, and the Sigma Xi Graduate Research Award from the University of Florida in 1999. He is a member of the Sensor Array and Multichannel (SAM) Technical Committee of the IEEE Signal Processing Society. He was an Associate Editor for the IEEE TRANSACTIONS ON WIRELESS COMMUNICATIONS (January 2003 to December 2006) and the IEEE SIGNAL PROCESSING LETTERS (January 2005 to December 2006), and has been an Associate Editor for the IEEE TRANSACTIONS ON SIGNAL PROCESSING since October 2006. He serves as a Guest Editor for the *EURASIP Journal on Applied Signal Processing* Special Issue on Distributed Signal Processing Techniques for Wireless Sensors Networks.